Classical dynamics of two-electron atoms at zero energy

Min-Ho Lee,[1] Nark Nyul Choi,[1] and Gregor Tanner[2]
[1]*School of Natural Science, Kumoh National Institute of Technology, Kumi, Kyungbook 730-701, Korea*
[2]*School of Mathematical Sciences, University of Nottingham, University Park, Nottingham NG7 2RD, United Kingdom*
(Received 22 August 2005; published 22 December 2005)

We give a complete description of the classical dynamics of two electrons in the Coulomb potential of a positively charged nucleus for total energy $E=0$ and angular momentum $L=0$. The effectively four-dimensional phase space can be divided into partitions spanned by the stable and unstable manifold of the Wannier ridge space. We identify a further approximate symmetry by choosing an appropriate Poincaré surface of section in this dynamical system. In addition, a dividing surface between the dynamics influenced by the two collinear spaces, the stable *Zee* space and the strongly chaotic *eZe* space can be identified. We discuss potential extensions of the binary symbolic dynamics found in collinear two-electron atoms to the noncollinear parts of the phase space for $E \leqslant 0$.

DOI: 10.1103/PhysRevE.72.066215 PACS number(s): 05.45.Mt, 45.50.−j, 34.10.+x

I. INTRODUCTION

Two electron atoms play a special role in atomic physics. On the one hand, the interaction strength between the three particles are all of the same order which limits the scope for perturbative approaches, especially for highly, doubly excited states. The small number of particles, on the other hand, as well as the long-range potentials makes mean-field approaches useless for large parts of the atomic spectrum above the ionisation threshold.

A valuable source of inspiration for a qualitative and quantitative theoretical analysis of quantum effects in two-electron atoms has recently emerged in the form of classical and semiclassical studies of the corresponding classical three-body Coulomb dynamics. Electron-electron correlation effects in double-ionisation processes [1] as well as the existence of approximate quantum numbers could be explained qualitatively in terms of properties of the underlying classical dynamics, see Ref. [2]. The fact that two-electron atoms show approximate symmetries has been established experimentally and in numerical quantum calculations and explained qualitatively by group theoretical arguments [3] and in terms of adiabatic invariants [4], see Ref. [2] for an overview. This suggests a related, but yet unknown symmetry in the corresponding classical problem. This symmetry can be associated with a stable bending type of motion of the correlated electron dynamics near collinear subspace of the full dynamics, that is, the *eZe* and *Zee* space (here, the name indicates the order in which the three particles are aligned) [2,5–11]. The dynamics in the neighbourhood of these two subspaces is, however, not compatible, which suggests the existence of a separatrix between *eZe*-like and *Zee*-like dynamics. A breakdown of the approximate quantum numbers is expected in this region which has indeed been seen in numerical calculations [12].

To unveil the classical origin of approximate symmetries in two-electron atoms, an analysis of the phase space dynamics beyond the known two degrees of freedom subspaces is essential. Recent progress in this direction has been reported in Refs. [13,14] where a full analysis of the dynamics near the triple collision for angular momentum $L=0$ has been presented. In particular, the behavior of the stable and unstable manifold of the triple collision has been studied in detail and self-similar structures in scattering data could be explained.

Already finding the a suitable Poincaré surface of section (PSOS) is a major problem in such high-dimensional dynamical systems. In this paper, we will suggest a PSOS which allows us to give an analysis of the effectively four-dimensional dynamics of the zero-energy phase space for $L=0$ which is complementary to the approach taken in Refs. [13,14]. This allows us to study directly the transition from the *eZe* to the *Zee* space and to show that the stable and unstable manifold of the so-called Wannier ridge provides a Markov partition in $E=0$. An associate symbolic dynamics can be directly linked to the well known binary Markov partition of the *eZe* space for $E<0$ [7,8]. The PSOS may thus prove valuable for an extension of the analysis to the physically much more interesting and challenging phase space for $E<0$.

II. BASIC EQUATIONS AND THE PSOS $\Pi_{\theta=\pi}^{E=0}$

In what follows, we will refer to the two-electron dynamics at the double-ionisation threshold $E=0$ for total angular momentum $L=0$ if not stated otherwise. The latter implies, that all three particles move in a plane. The Hamiltonian in the infinite-nucleus mass approximation can in appropriate units be written as

$$H=\frac{\mathbf{p}_1^2}{2}+\frac{\mathbf{p}_2^2}{2}-\frac{Z}{r_1}-\frac{Z}{r_2}+\frac{1}{r_{12}}=0, \tag{1}$$

where Z refers to the charge of the nucleus and r_1, r_2, r_{12} are the electron-nucleus and electron-electron distances. We will consider helium, that is $Z=2$, if not stated otherwise.

We will work in hypersphercial coordinates, that is, we introduce the hyperradius $R=\sqrt{r_1^2+r_2^2}$, the hyperangle $\alpha=\tan^{-1}(r_2/r_1)$ and the interelectronic angle $\theta=\angle(\mathbf{r}_1,\mathbf{r}_2)$. By employing a McGehee transformation [15] of the form

$$\bar{\alpha} = \alpha, \quad \bar{\theta} = \theta, \quad \bar{R} = \frac{1}{R} R = 1,$$

$$\bar{p}_R = \sqrt{R} p_R, \quad \bar{p}_\alpha = \frac{1}{\sqrt{R}} \sqrt{\sin\alpha \cos\alpha} p_\alpha,$$

$$\bar{p}_\theta = \frac{1}{\sqrt{R}} \frac{1}{\sqrt{\sin\alpha \cos\alpha}} p_\theta,$$

$$d\bar{t} = \frac{1}{R^{3/2}} dt, \quad \bar{H} = \bar{E} = RE \tag{2}$$

and rewriting the equations of motion in the new coordinates, one obtains $\dot{\bar{H}}=0$ both for $E=0$ or $R=0$, thus reducing the phase space to effectively four dimensions [8,13]. The dynamics for $E=0$ is therefore equivalent to a dynamics at the triple collision point $R=0$ and appropriate coordinates are $\alpha, \theta, p_R, p_\alpha, p_\theta$ together with the constraint

$$\bar{H} = \frac{1}{2}\left(p_R^2 + \frac{p_\alpha^2 + p_\theta^2}{\sin\alpha \cos\alpha} \right) - Z \frac{\cos\alpha + \sin\alpha}{\sin\alpha \cos\alpha} + \frac{1}{\sqrt{1 - 2\cos\alpha \sin\alpha \cos\theta}} = 0. \tag{3}$$

We dropped the bar notation here again for convenience, except for $\bar{H}$. Note that the scaling for p_α and p_θ differs from the one defined in Refs. [13,14] and is chosen here to regularize the coordinates at the two-body collisions $\alpha=0$, $\pi/2$, that is, the momenta take on finite values at these points [16]. Furthermore, for $E=0$ one obtains $\dot{p}_R \geqslant 0$, that is, the p_R coordinate is monotonically increasing in time.

In the scaled dynamics, there are two fixed points at

$$\alpha = \pi/4, \quad \theta = \pi, \quad p_\alpha = 0, \quad p_\theta = 0,$$

$$p_R = \pm \sqrt{\sqrt{2}(4Z - 1)} = \pm P_0,$$

the triple collision point (TCP) with $p_R=-P_0$ and its time reversed partner, the double escape point (DEP) with $p_R=P_0$ corresponding in unscaled coordinates to a two-electron trajectory approaching or escaping the nucleus symmetrically along $\theta=\pi$. There are no periodic orbits in the system due to $\dot{p}_R \geqslant 0$. There are, however, three invariant subspaces of the dynamics: the collinear spaces $\theta=\pi$, $p_\theta=0$ (the *eZe* configuration) and $\theta=0$, $p_\theta=0$ (the *Zee* configuration) and the so-called Wannier ridge (WR) of symmetric electron dynamics with $\alpha=\pi/4$, $p_\alpha=0$. Note that the fixed points lie at the intersection of the *eZe* and the WR spaces.

For completeness, we also give the discrete symmetries of the system, that is, particle exchange, inversion, and time-reversal symmetry in the new coordinates. The Hamiltonian and the equations of motion are invariant under the transformations

particle exchange:

$$(\alpha, \theta, p_R, p_\alpha, p_\theta) \to (\pi/2 - \alpha, -\theta, p_R, -p_\alpha, -p_\theta),$$

inversion:

$$(\alpha, \theta, p_R, p_\alpha, p_\theta) \to (\alpha, -\theta, p_R, p_\alpha, -p_\theta),$$

time reversal:

$$(\alpha, \theta, p_R, p_\alpha, p_\theta) \to (\alpha, \theta, -p_R, -p_\alpha, -p_\theta).$$

In Refs. [13,14], an analysis of the dynamics in the $E=0$ space is given using the PSOS defined as $\theta=\pi$ which will be denoted by $\Pi_{\theta=\pi}^{E=0}$. The boundary of the PSOS is the *eZe* phase space in $E=0$. Note that Fig. 1(a) differs from the one presented in, e.g., Refs. [8,14] at $\alpha=0$ or $\pi/2$ due to the different scaling chosen for the momenta.

The PSOS consists actually of two sheets corresponding to either $p_\theta>0$ and $p_\theta<0$ on the PSOS; only one sheet is shown in Fig. 1(a). The two sheets can be mapped onto each other by the inversion symmetry and are connected at the binary collision planes $\alpha=0$ and $\pi/2$, the shaded areas in Fig. 1(a). Furthermore, on the *eZe* boundary, a point (α, p_α) on the $p_\theta>0$ sheet is identical to its counterpart on the $p_\theta<0$ due to $p_\theta=0$ there. That is, the boundary belongs actually to both sheets. There is, however, no flux across the boundary as it is an invariant subspace of the dynamics.

We will briefly turn to the binary collisions planes restricting the discussion to $\alpha=0$ in what follows. From Eq. (3), one obtains

$$p_\alpha^2 + p_\theta^2 = 2Z$$

at a binary collision independent of p_R. The values of p_α are thus between $\pm\sqrt{2Z}$ with $p_\alpha = \pm\sqrt{2Z}$ on the *eZe* boundary. Other points in $\alpha=0$ correspond to binary collisions with an interelectronic angle $\theta \neq \pi$ near the collision. Note in particular, that $p_\alpha=0$ is part of the *Zee* subspace. For near collision trajectories, the colliding electron makes a 2π turn around the nucleus, see Fig. 2; binary collision trajectories are thus self-retracing in the limit $\alpha \to 0$ and initial conditions p_α, p_θ on $\alpha=0$ are identical to their time reversed partners $-p_\alpha, -p_\theta$. This means in particular, that the two sheets of $\Pi_{\theta=\pi}^{E=0}$ are continuously connected at the binary collision planes as stated earlier once we make the identification $(p_\alpha, p_\theta) \equiv (-p_\alpha, -p_\theta)$ at $\alpha=0$.

The PSOS cuts through the WR and contains both fixed points. $\Pi_{\theta=\pi}^{E=0}$ is therefore ideally suited to study the connection between the various stable and unstable manifolds of the fixed points. In fact, the WR forms a heteroclinic connection between the TCP to the DEP; this, together with the topology of the $E=0$ phase space leads to a characteristic foliation of the three-dimensional stable manifold S_D of the DEP as it progresses from $p_R \to -\infty$ toward the DEP. (By time reversal symmetry, the same holds for the unstable manifold U_T of the TCP.) This leads to a five-leaves structure of the S_D for $p_R < -P_0$, that is, five distinct pieces of the S_D come arbitrarily close to the 1D stable manifold S_T of the TCP in $E=0$, as described in detail in Ref. [14].

This mechanism has a big effect on classical scattering for $E<0$; the DEP acts as an entrance gate to chaotic scattering,

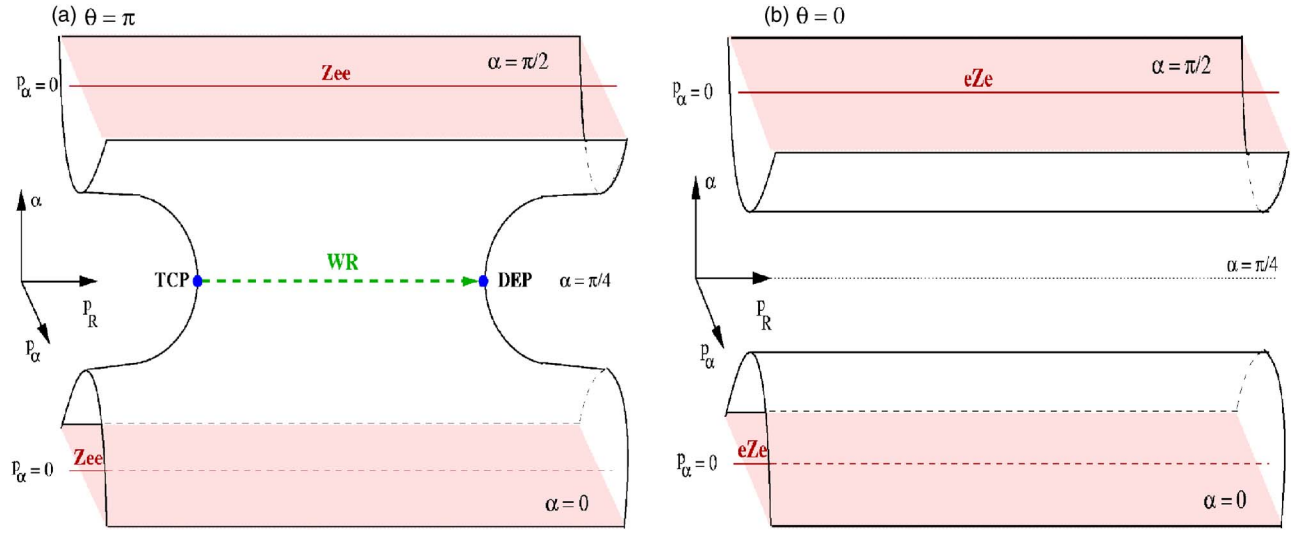

FIG. 1. (Color online) The PSOS $\theta=\pi$ (a) and $\theta=0$ (b) in $\alpha-p_\alpha-p_R$ coordinates for $E=0$. Only the sheet for $p_\theta \geqslant 0$ is shown in both cases.

that is, only those trajectories approaching the nucleus close to the S_D can enter a chaotic scattering region. They do so along the five leaves forming five distinct paths into the chaotic region, which can clearly be seen in numerical scattering signals such as the scattering time plots presented in Ref. [14]. In fact, for $E<0$ another connection between the two fixed points emerges; the unstable manifold of the DEP in the *eZe* subspace coincides with the stable manifold of the TCP along the so-called Wannier orbit (WO) with $\alpha=\pi/4$, $\theta=\pi$, $p_\alpha=p_\theta=0$ in $E<0$. This leads to a conveyor belt mechanism along which trajectories can be transported back and forth between the two fixed points and can thus reenter the chaotic scattering region leading to self-similar patterns in the scattering signal [14].

The PSOS $\Pi_{\theta=\pi}^{E=0}$ is not very well suited for analysing the transition from the *eZe* to the *Zee* subspace or for studying the possibility of a global symbolic dynamics. In fact, the Markov partition associated with the binary symbolic dynamics in *eZe* is defined with respect to the binary collision planes [7,8] and so is the dynamics near *Zee* in $\Pi_{\theta=\pi}^{E=0}$. To separate these dynamical features, it is advantageous to switch to a different PSOS. An ideal candidate is the PSOS $\theta=0$ which will be discussed in the next section [17].

III. THE PSOS $\Pi_{\theta=0}^{E=0}$

The PSOS $\Pi_{\theta=0}$ is defined by the condition $\theta=0$ in the full phase space $E\leqslant 0$. We will in the following mainly restrict ourselves to $\Pi_{\theta=0}^{E=0}$ defined on $E=0$. The boundary of the PSOS is now formed by the *Zee* space and consists of two disconnected parts separated by the *e-e* repulsion peak in the potential at $\alpha=\pi/4$, see Fig. 1(b). Again, we plot here only the $p_\theta>0$ section of the PSOS; the two sheets $p_\theta>0$ and $p_\theta<0$ are connected at the binary collision planes $\alpha=0$ or $\pi/2$ in the same way as outlined for $\Pi_{\theta=\pi}^{E=0}$. The full PSOS consists thus of two disconnected cylinders centered at $\alpha=0$, $p_\alpha=0$ and $\alpha=\pi/2$, $p_\alpha=0$. The two parts are related by the particle exchange symmetry and the dynamics can be restricted to only one of the components by symmetry reduction [7].

In what follows, we will discuss only the lower part of the PSOS in Fig. 1(b), that is, $\alpha<\pi/4$. The two halves of the cylinder are connected at $\alpha=0$ due to the identification $p_\alpha \equiv -p_\alpha$, $p_\theta \equiv -p_\theta$ in that plane in the same way as described in Sec. II, see Fig. 2. The dynamics in the two halves is related by inversion symmetry, and we will often only consider the $p_\theta>0$ part of $\Pi_{\theta=0}^{E=0}$. Note that $\alpha=0$, $p_\alpha=0$ corresponds to the *eZe* space; $\Pi_{\theta=0}^{E=0}$ thus provides a PSOS topologically equivalent to a cylinder which contains both collinear subspaces spatially well separated, the *eZe* space as the axis and the *Zee* space as its surface. [Note, that on the *Zee* surface, points (α,p_α) are identical on both halves.] It is natural to parametrise the PSOS in cylindrical coordinates p_R,ρ,ϕ which for each half may be written as

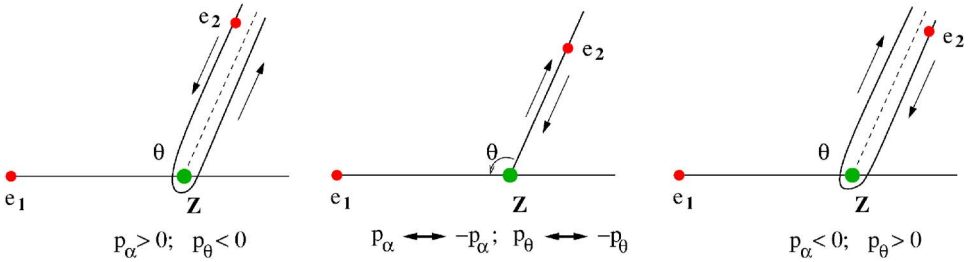

FIG. 2. (Color online) Dynamics near binary collisions with respect to an angle θ. The trajectories become self-retracing at the collision leading to an identification $(p_\alpha,p_\theta)\equiv(-p_\alpha,-p_\theta)$ at $\alpha=0$ or $\pi/2$.

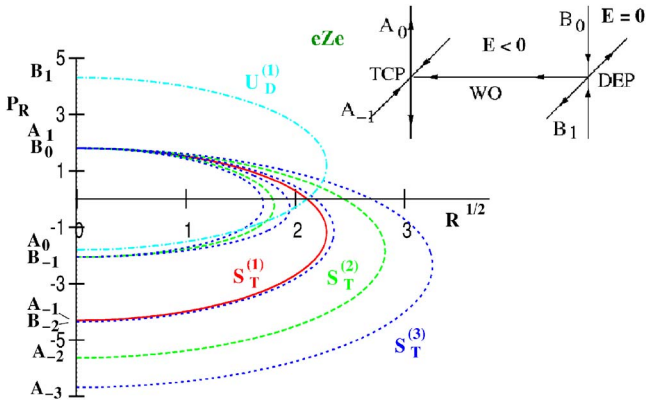

FIG. 3. (Color online) The partition generating the binary symbolic dynamics in the *eZe* space. The one-dimensional map f is defined on $R=0$ or equivalently on $E=0$. Here, $S_T^{(n)}$ denotes that part of the stable manifold of the TCP which reaches the triple collision after n steps. Likewise, $U_D^{(n)}$ is the nth generation of the unstable manifold of the DEP.

$$\alpha = \rho g(p_R,\phi)\cos\phi, \quad p_\alpha = \rho g(p_R,\phi)\sin\phi. \tag{4}$$

Here $g(p_R,\phi)>0$ is chosen such that the radial coordinate $\rho\in[0,1]$ and $\phi\in[-\pi/2,\pi/2]$. Before turning to the symbolic dynamics in $\Pi_{\theta=0}^{E=0}$, we need to review some aspects of the symbolic dynamics in the *eZe* space, which will be done in the next section.

A. The symbolic dynamics in the *eZe* space

In *eZe* the symbolic dynamics is defined with respect to the PSOS $\alpha=0$ after symmetry reduction, which will be denoted $\Pi_{\alpha=0}^{eZe}$ [7]. The PSOS's $\Pi_{\theta=0}^{E=0}$ and $\Pi_{\alpha=0}^{eZe}$ intersect along the line $\rho=0$ in $E=0$, see Figs. 1(b) and 3. The one-dimensional Poincaré map defined on $\rho=0$ may be written in the form

$$p_R^{(n+1)} = f(p_R^{(n)}), \tag{5}$$

where f is a monotonically increasing function [8]. Of special interest are here the intersections of the stable and unstable manifolds of the two fixed points TCP and DEP, with the $\Pi_{\alpha=0}^{eZe}$; let A_i, $i<0$ be the intersections of the S_T with the $\Pi_{\alpha=0}^{eZe}$ in $E=0$ such that A_{-1} is the point from which the S_T leads directly into the TCP fixed point. In the same way, A_i, $i\geqslant 0$ are the points at which the U_T intersects $\Pi_{\alpha=0}^{eZe}$ in $E=0$; we identify $f(A_{-1})=A_0$ which continues the map across A_{-1} in a natural way. Analogously, B_i are the intersections of the invariant manifolds of the DEP with the PSOS such that B_i is part of the S_D for $i\leqslant 0$ and of the U_D for $i>0$. We make again the identification $f(B_0)=B_1$; note that $B_i=-A_{-i}$ by time reversal symmetry [18], see Fig. 3 along the axis $R=0$.

An appropriate symbolic dynamics for the full *eZe* space is given by the condition

0 if $\alpha\neq\pi/4$ between subsequent binary collisions,

1 if $\alpha=\pi/4$ between subsequent binary collisions. (6)

For the map f, this rule is equivalent to assigning a symbol 1 to initial conditions in $A_{-1}<p_R<B_0$ and 0 otherwise. The possible admissible symbol sequences in the *eZe* space for $E=0$ is limited; in particular, for the physically relevant cases $Z\geqslant 1$ and large nucleus/electron mass ratios [8,11], only two types of sequences occur, namely,

$$\cdots 0001100\cdots \quad \text{for } p_R\in(A_i,B_i),$$
$$\cdots 0001000\cdots \quad \text{for } p_R\in(B_i,A_{i+1}).$$

For $E<0$, a complete binary symbolic dynamics emerges in *eZe*; this is due to the fact that the S_T coincides with the U_D along the Wannier orbit (WO). Points close to B_0 are thus mapped both onto B_1 as well as A_0; similarly, A_0 can be reached both from A_{-1} and B_0, see inset in Fig. 3. In fact, the Poincaré map associated with $\Pi_{\alpha=0}^{eZe}$ can no longer be continued across the points A_0 and B_0 as was the case in the 1D map (5); instead, the whole S_T including A_{-1} and B_0 are mapped onto A_0; similarly, B_0 is the preimage of the U_D including both B_1 and A_0. This creates the folding mechanism necessary for providing the partition of the full $\Pi_{\alpha=0}^{eZe}$ in terms of the two-dimensional manifolds S_T and U_D as shown in Fig. 3, see Refs. [7,8] for details. We will come back to this partition in Sec. III C; first, we will discuss an extension of this symbolic dynamics into the full $E=0$ space.

B. The symbolic dynamics in $\Pi_{\theta=0}^{E=0}$

We propose to generalise the *eZe* symbolic dynamics to the full $E=0$ space with respect to $\Pi_{\theta=0}^{E=0}$ such that

$$\text{symbol } n \Leftrightarrow n \text{ crossings of } \alpha=\pi/4$$

in one step of the associate Poincaré map. The manifold generating the partition is the stable manifold of the Wannier ridge, S_W. This manifold consists of the three-dimensional S_D together with the one dimensional S_T (which is a boundary of the S_D [14]). Only those trajectories converging to the WR will not return to the $\Pi_{\theta=0}^{E=0}$. The qualitative difference in the behavior on either side of the partition is shown in Fig. 4 depicting a swarm of trajectories in the α-θ plane starting on the $\Pi_{\theta=0}^{E=0}$ with $p_\theta>0$. The symbol codes in the left panel are $\cdots 0.110\cdots$ and $\cdots 0.10\cdots$, where the dot in the symbol code represents the position for a given initial condition. (Thus, $\cdots 0.110\cdots$ refers to an initial condition which will lead to symbols 1 in the next two steps; the ellipses indicate infinite strings of symbols 0.) Similarly, we have $\cdots 0.20\cdots$ and $\cdots 0.10\cdots$ on the right-hand part of Fig. 4 due to the fact that the trajectories cross the line $\alpha=\pi/4$ once or twice in one step of the Poincaré map. The dividing trajectory is in each case on the S_W converging to the DEP $\alpha=\pi/4$, $\theta=\pi$.

In fact, the $\Pi_{\theta=0}^{E=0}$ defines a three-dimensional map for which the coordinate p_R increases monotonically in time similar to the one-dimensional map f in Eq. (5). The S_W provides a partition of the space in the sense that sections of the S_W in the $\Pi_{\theta=0}^{E=0}$ are mapped onto each other in accordance to their end points A_i and B_i on the p_R axis. The most striking feature is, however, the regularity of the partition with re-

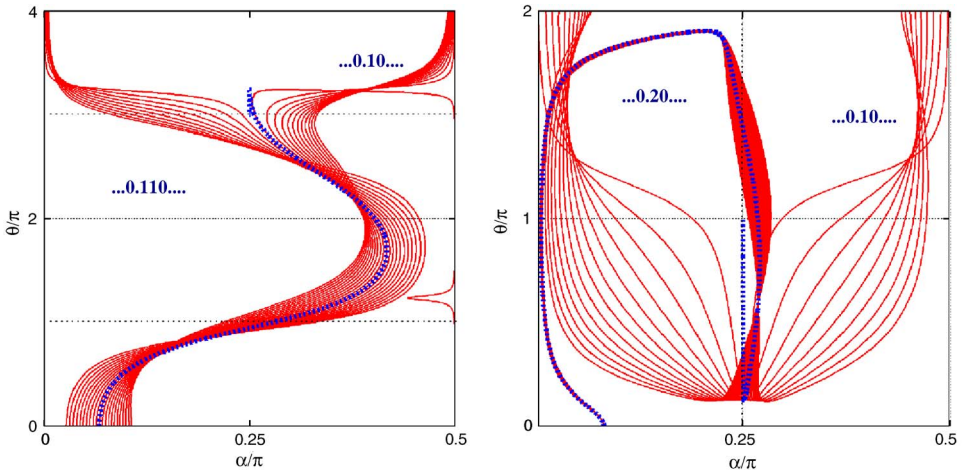

FIG. 4. (Color online) Swarm of trajectories starting on $\Pi_{\theta=0}$; the thick, dashed line divides the swarm into trajectories with different symbol code and lies on the S_W converging to the DEP at $\alpha=\pi/4$, $\theta=\pi$.

spect to a change in the angle ϕ defined in Eq. (4). The $\Pi_{\theta=0}^{E=0}$ unveils an approximate rotational symmetry in the $\alpha-p_\alpha$ coordinates. In Fig. 5, the S_W is shown in cuts through the $\Pi_{\theta=0}^{E=0}$ for different angles ϕ. The origin of the cylindrical coordinates is the p_R axis at $\rho=0$ which is nothing but $\Pi_{\alpha=0}^{eZe}$ restricted to $E=0$. The *Zee* space forms the outer boundary which is here rescaled to $\rho=1$ using (4). In Fig. 5, a more or less uniform behaviour is observed for angles in the regime $-0.97<\phi/\pi/2<0.76$. The time reversed partner of the S_W, the U_W, is obtained by the symmetry operation $p_R\rightarrow -p_R$ and $\phi\rightarrow-\phi$; the first part of the U_W starting at A_0 is also shown in Fig. 5. Note, that the five leaves structure emerges out of the S_T at points A_i, $i<0$ as well as at B_i, $i>0$ at the U_D.

The S_W and U_W provide a partition of the PSOS. Essentially, 4 different regions emerge, each mapped onto itself under the Poincaré map. This is depicted in Fig. 6, which is an enlarged version of the cut at $\phi=0$ in Fig. 5. In terms of the symbolic dynamics these regions can for $p_R<B_{-1}$ and $A_1<p_R$ be labeled as

$\cdots 000\cdots$ bounded by *Zee* and (S_W or U_W),
$\cdots 010\cdots$ bounded by (B_i,A_{i+1}) and (S_W or U_W),
$\cdots 0110\cdots$ bounded by (A_i,B_i) and (S_W or U_W),
$\cdots 020\cdots$ bounded by S_W or U_W only.

Compared to the 1D map f in Eq. (5), there are two new regions. The first is the region $\cdots 020\cdots$ which is completely surrounded by the leaves of the S_W emerging from the S_T at points A_i, $i<0$. It originates from the folding mechanism of the S_W described in Refs. [13,14]. Trajectories in this region cross the line $\alpha=\pi/4$ twice while traversing the interval $A_0<p_R<B_0$, see Fig. 4; the corresponding parts of this region for $p_R>0$ are bounded by the U_W emerging from points B_i, $i>0$. The second region $\cdots 000\cdots$ borders onto the *Zee* boundary and approaches the *eZe* subspace only in a narrow strip between the leaves of the S_W or U_W at points A_i, $i<0$ or B_i, $i>0$, respectively. The S_W and U_W thus provide a natural boundary between the *eZe* and the *Zee* spaces at least in the limit $E\rightarrow 0$. This is of importance for understanding the range of validity of approximate quantum numbers in two-electron atoms and the transition between quantisation schemes based on the dynamics in the neighborhood of the collinear subspaces [2].

The dynamics of the $\cdots 010\cdots$ and $\cdots 0110\cdots$ regions are more or less similar to the 1D case for $\Pi_{\alpha=0}^{eZe}$ restricted to $E=0$, see Fig 3. It remains to be added that the $\cdots 01.10\cdots$ region is bounded by the interval $[A_0,B_0]$ and the S_W as well as the U_W up to the crossing point C in Fig. 6. Similarly, $\cdots 0.10\cdots$ comprises the area bounded by $[B_{-1},A_0]$ as well as the S_W and U_W. In fact, as in the *eZe* partition for $E<0$, the Poincaré map can no longer be uniquely continued at points A_{-1} and B_1 which end in or come out of the triple collision. Instead, the image of A_{-1} must be identified with the whole U_D bounded by A_0 and B_1; A_{-1} is in particular also mapped onto C. In the same way, the whole two-dimensional S_D in $\Pi_{\theta=0}^{E=0}$ may be identified by being eventually mapped onto the point B_1 which is part of the U_D.

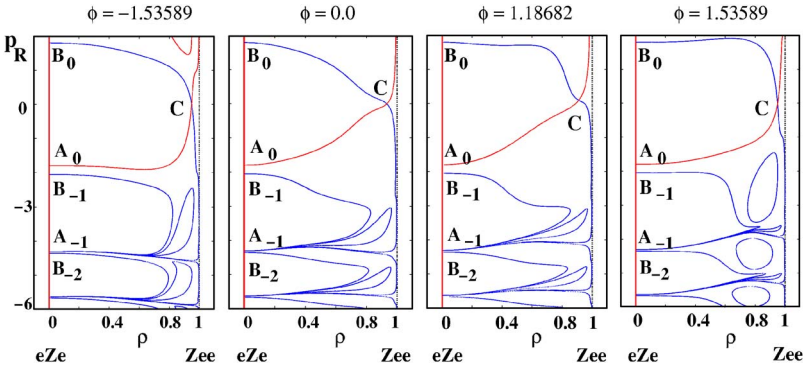

FIG. 5. (Color online) Cuts through the $\Pi_{\theta=0}^{E=0}$ along $\phi=$const together with the invariant manifolds of the WR.

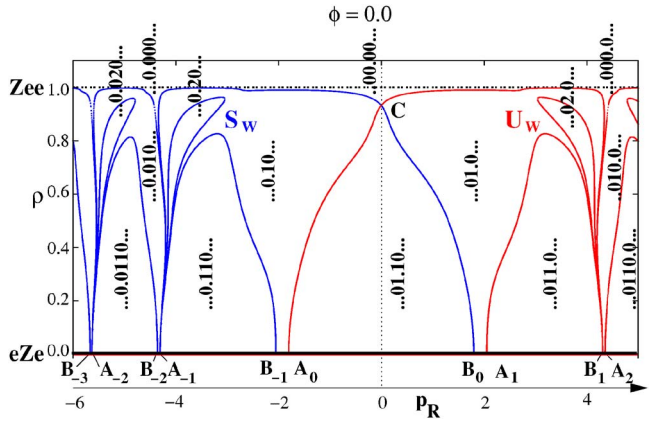

FIG. 6. (Color online) Cut through the $\Pi_{\theta=0}^{E=0}$ along $\phi=0$, that is $p_\alpha=0$ together with the partition due to the S_W and U_W and the associate symbolic coding.

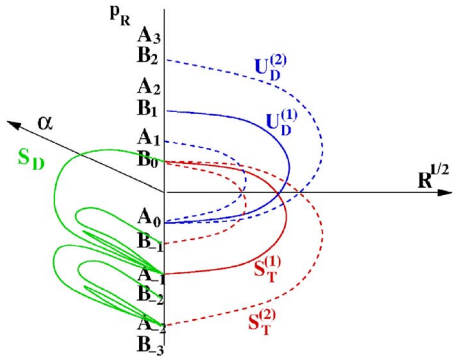

FIG. 7. (Color online) Extension of the manifold structure to the full $\Pi_{\theta=0}$; note that at $R=0$ the cut $p_\alpha=0$ is chosen (schematic drawing).

C. Extensions to $E<0$

The rotational symmetry of $\Pi_{\theta=0}^{E=0}$ makes it possible to discuss the full PSOS $\Pi_{\theta=0}$. Putting the Poincaré cuts from Figs. 3 and 6 together, we end up with a scenario as sketched in Fig. 7. We stress that the $\Pi_{\theta=0}^{E=0}$ is three dimensional, the full PSOS for $E\leqslant 0$ (or $R\geqslant 0$) is thus four dimensional. However, any cut in $E=0$ with constant angle ϕ gives a similar picture which indicates that it may be possible to study the full $\Pi_{\theta=0}$ in a three-dimensional cut as indicated in Fig. 7, (here for $p_\alpha=0$, that is, $\phi=0$). A smooth continuation from the complete binary symbolic dynamics in the *eZe* space to the symbolic coding in $\Pi_{\theta=0}^{E=0}$ becomes apparent. An additional complication arises due to the five leaves structure emerging from the stable and unstable manifolds $S_T^{(n)}$ and $U_D^{(n)}$ when considering $\alpha>0$. These leaves transform into a self-similar chaotic scattering region due to the conveyor belt mechanism discussed briefly in Sec. II. We will not enter into a detailed analysis of a possible extension of the symbolic dynamics to the full phase space; this is indeed part of ongoing studies at the moment. We hope, however, that Fig. 7 helps to visualise how the different parts of these high-dimensional Poincaré cuts join together and why an extension of the self-similar structure related to a binary symbolic dynamics is so robust even far from the *eZe* space as reported in Ref. [14]. The new PSOS $\Pi_{\theta=0}$ is also helpful to identify the separatrix between *eZe*- and *Zee*-like behavior in the dynamics at least in the limit $E\to 0$. We note that the S_W can in principle provide a dividing surface in the full four-dimensional $\Pi_{\theta=0}$; it is, however, no longer a nice, simple surface but undergoes a complicated folding pattern related to the conveyor belt mechanism. Still the S_W seems a very promising candidate for a global partition.

IV. CONCLUSIONS

The dynamics in the PSOS $\Pi_{\theta=0}^{E=0}$ has been analysed in detail; the PSOS makes it possible to discuss the partition of the phase space in terms of the stable and unstable manifold of the Wannier ridge, the S_W and U_W. We identify a symbolic dynamics which matches smoothly onto the binary symbolic dynamics in the *eZe* space reached here in the limit $\rho\to 0$ and $E\to 0$. It becomes apparent that the S_W and U_W act as a separatrix between neighborhoods of the *Zee* and *eZe* spaces, a fact which will be important in understanding the breakdown of approximate symmetries and associated quantum numbers in quantum treatment of the problem.

ACKNOWLEDGMENTS

N.N.C. thanks the Korea Research Foundation (Grant No. KRF-2003-015-C00119) for financial and the KISTI supercomputing center for numerical support. Parts of this work were carried out at *MPI for Complex Systems* in Dresden which we would like to thank for its hospitality.

[1] G. H. Wannier, Phys. Rev. **90**, 817 (1953); J. M. Rost, Phys. Rep. **297**, 271 (1998); R. Doerner *et al.*, *ibid.* **330**, 95 (1998); Th. Weber *et al.*, Nature (London) **405**, 658 (2000); B. Eckhardt and K. Sacha, Phys. Scr. **T 90**, 185 (2001); T. Schneider and J. M. Rost, Phys. Rev. A **67**, 062704 (2003).
[2] G. Tanner, K. Richter, and J. M. Rost, Rev. Mod. Phys. **72**, 497 (2000).
[3] D. A. Herrick, Adv. Chem. Phys. **52**, 1 (1983).
[4] J. M. Feagin and J. S. Briggs, Phys. Rev. Lett. **57**, 984 (1986).
[5] K. Richter and D. Wintgen, Phys. Rev. Lett. **65**, 1965 (1990).
[6] G. S. Ezra, K. Richter, G. Tanner, and D. Wintgen, J. Phys. B **24**, L413 (1991).
[7] K. Richter, G. Tanner, and D. Wintgen, Phys. Rev. A **48**, 4182 (1993).
[8] Z.-Q. Bai, Y. Gu, and J. M. Yuan, Photochem. Photobiol. **118**, 17 (1998).
[9] B. Duan, Z. Bai, and Y. Gu, Phys. Rev. A **61**, 062711 (2000).
[10] R. Puttner, B. Gremaud, D. Delande, M. Domke, M. Martins,

A. S. Schlachter, and G. Kaindl, Phys. Rev. Lett. **86**, 3747 (2001).
[11] M. M. Sano, J. Phys. A **37**, 803 (2004).
[12] A. Bürgers, D. Wintgen, and J-M. Rost, J. Phys. B **28**, 3163 (1995).
[13] N. N. Choi, M.-H. Lee, and G. Tanner, Phys. Rev. Lett. **93**, 054302 (2004).
[14] M.-H. Lee, G. Tanner, and N. N. Choi, Phys. Rev. E **71**, 056208 (2005).
[15] R. McGehee, Invent. Math. **27**, 191 (1974).
[16] Note that this leads to a regularization of the coordinates only; the equations of motion are still singular at two-body collisions. To obtain a set of non-singular equations of motion, a combined McGehee-Kustanheimo-Stiefel transformation needs to be employed as in Ref. [14].
[17] The sections $\alpha=0$ and $\pi/2$ itself are in fact not good PSOS's; trajectories coming close to $\alpha=0$ will do so by swirling round the nucleus once and thus asymptotically covering the whole θ interval $[0,2\pi]$ for $\alpha\to 0$, see Fig. 2. This means that the space $\alpha=0$ is tangential to the flow, which in turn implies that binary collisions are rare events, that is, a typical trajectory will not hit $\alpha=0$.
[18] Our notation of the points A_i, B_i deviates slightly from Ref. [8]; one finds $A_i'=A_{-i-1}$ and $B_i'=B_{-i}$ where the primed notation is the one used in Ref. [8].